J Mater Sci (2008) 43:1795–1801
DOI 10.1007/s10853-007-2381-4

Temperature-dependent refractive index of semiconductors

Nicolas Cherroret · Abhijit Chakravarty · Aravinda Kar

Received: 12 August 2007 / Accepted: 4 December 2007 / Published online: 18 January 2008

Abstract A single-oscillator Lorentz model is applied to four different semiconductors having diamond-like crystal structure to describe the temperature dependence of their refractive index between 300 and 600 K. Theoretical results are compared to previous experiments and to experiments carried out in this study for Si, Ge, GaAs, and InP. An efficient experimental method is also presented, enabling fast measurements of the refractive index of materials. Using the Yu-Brooks formalism and the energy bandgap at the X-point of the Brillouin zone, the temperature-dependent refractive indices are calculated and they agree well with experiments, particularly, considering the simplicity of the Lorentz model. However, there are discrepancies between the theory and experiment at high temperatures (near 600 K) in certain cases. This discrepancy may be due to the single-oscillator approximation. Additionally the effect of "self-energy" on the temperature dependence of the energy bandgap, such as the temperature-dependent damping of the oscillation of electrons, can be significant at higher temperatures.

N. Cherroret
Ecole Nationale Supérieure de Physique de Grenoble (ENSPG), St-Martin d'Hères 38402, France

A. Chakravarty (✉)
Department of Electrical Engineering and Computer Science, Laser-Aided Manufacturing, Materials and Micro-Processing Laboratory (LAMMMP), College of Optics and Photonics/ CREOL, University of Central Florida, Orlando FL 32816-2700, USA
e-mail: abhijit_chakravarty2002@yahoo.com

A. Kar
Department of Mechanical, Materials and Aerospace Engineering, College of Optics and Photonics, Center for Research and Education in Optics and Lasers (CREOL), University of Central Florida, Orlando, FL 32816-2700, USA

Introduction

The knowledge of the refractive index of solids and especially semiconductors is of fundamental interest in diverse fields such as optical instrumentation and optoelectronics. The temperature dependence of this physical quantity has often been studied experimentally and very few theoretical models exist on this subject because the interaction of lasers with solids is generally difficult to describe quantitatively at high temperatures. The variation of the refractive index with temperature is based on the thermo-optic effect in which the phonons and electrons modify the refractive index at different temperatures, affecting the interaction of light with the material.

The purpose of this work is to present two meaningful models based on the Lorentz model of dielectrics and the works of Yu and Cardona [1] and Fan [2], in order to obtain theoretical expressions for refractive index over a wide range of temperatures (300–600 K). These models are generally used to calculate the average values of the thermo-optic coefficient dn/dT and rarely to analyze the temperature dependence of refractive index. The theoretical model of this work is compared with experimental data for four semiconductors such as Si, Ge, GaAs, and InP each of which has diamond-like crystal structure. Also lights of wavelength in the near infrared or the visible range are considered to examine only the electronic contribution to the thermo-optic effect.

Physical and mathematical model

The thermo-optic effect is a weak phenomenon which is difficult to model. This weak phenomenon, however, has tremendous impacts on a variety of high-technology

applications such as optical communications and spectral stability of lasers in resonators. Noting the simplicity of the classical Lorentz model, this model has been used in the present work by considering temperature-dependent material properties to understand the variation of refraction index (n) with temperature (T), i.e., $n(T)$.

Single-oscillator model for $n(T)$

The model is developed in this study for wavelengths 1523, 1900, and 623.8 nm. The first two values belong to the near infrared range and the last one to the visible range of the electromagnetic spectrum. The electronic polarization mechanism is dominant in this range compared to the ionic polarization mechanism. So the ionic contribution to the polarization can be neglected. Besides, the ionic contribution is quite weak—although a little stronger in GaAs and InP than in Si and Ge—in these semiconductors since the thermo-optic coefficients are generally positive.

Considering bound and free electrons in semiconductors, the multi-oscillator model provides the following expression for the refraction index [3]

$$n^2 = 1 + \sum_{\substack{j=1 \\ bound}}^{p'} \frac{N_1 e^2}{\varepsilon_0 m} \frac{f_j}{\omega_{0j}^2 - \omega^2} \tag{1}$$

by neglecting the damping effect for valence electrons and the local field effects. ω_{0j} corresponds to the j-th resonant frequency of an atom and f_j to the corresponding oscillator strength. This expression of $n(T)$ is applied to the above-mentioned four types of semiconductors.

Equation 1, however, is still very complicated because every resonant frequency of an atom is generally unknown especially at high temperatures. So a single-oscillator model is adopted to write Eq. 1 in the following form expressing the electronic refractive index as

$$n^2 = 1 + \frac{\omega_p^2}{\omega_0^2 - \omega^2} \tag{2}$$

where ω_p is the electronic plasma frequency and ω_0 an "average" resonant frequency. To estimate this average resonant frequency, $\hbar.\omega_0$ is considered to be an energy bandgap E_g. Following the work of Yu and Cardona [1], we chose for $\hbar.\omega_0$ the energy gap at the X-point of the Brillouin zone, which is close to the energy corresponding to the strongest peak in the reflectivity spectrum of the group IV and group III-V semiconductors. The plasma frequency ω_p is given by $\omega_p = \sqrt{Ne^2/(\varepsilon_0 m)}$, where N is the number of electrons per unit volume, e is the electronic charge, ε_0 is the permittivity of free space, and m is the mass of an electron. Based on these relations, the following expression for the thermo-optic coefficient, dn/dT, can be obtained from Eq. 2:

$$\frac{dn}{dT} = \frac{n^2 - 1}{2n}\left(-3\alpha(T) - \frac{2}{E_g}\frac{1}{1 - \frac{E_g^2}{E_g^2}}\frac{dE_g}{dT}\right) \tag{3}$$

where $\alpha(T)$ is the linear thermal expansion coefficient. Equation 3 shows that the refractive index of a dielectric material depends on temperature due to two basic properties of the material, the thermal expansion and the temperature dependence of the energy bandgap. In semiconductors and more generally in a few ionic materials, the effect of the bandgap shift on dn/dT is dominant and the thermo-optic coefficient is, therefore, positive. The temperature dependence of the energy bandgap is, however, difficult to obtain although the values of $\alpha(T)$ are generally well known (Table 1).

Bandgap shift due to the electron–phonon interactions

The electron–phonon interactions, which modify the band structure as the temperature changes, are considered to be the dominant mechanism for the shift in the energy bandgap. Two models for such interactions are reviewed below.

The "Fan" model

A model that will be used first to describe the electron-phonon interactions is due to Fan [2]. It is based on quantum mechanical interactions between the incident light and the electrons and phonons evaluated using a perturbation theory. Although this model is adapted to insulators, it can be extended to metals and monatomic semiconductors with a good approximation [10]. For nonpolar crystals such as Si and Ge, an expression of the variation of the gap with the temperature can be obtained [2, 11] as

$$(\Delta E_g)_{electron-lattice} = -2\frac{3}{q_D^3 M\hbar v_s} \sum_{\mp} \int_0^{q_D} \left(m_c^* C_c^2 \frac{n_q + \frac{1}{2} \mp \frac{1}{2}}{q \mp \frac{2v_s m_c^*}{\hbar}} + m_v^* C_v^2 \frac{n_q + \frac{1}{2} \mp \frac{1}{2}}{q \mp \frac{2v_s m_v^*}{\hbar}} \right) q^2 dq \tag{4}$$

In Eq. 4, M is the ionic mass which can be taken as the atomic mass to first approximation. v_s is the sound velocity of longitudinal phonons and q_D is the Debye wave vector. The determination of deformation potentials for the valence and the conduction bands C_v and C_c is generally a complicated problem. For our calculations, we consider them equal and chose their values as the hydrostatic deformation potential at the X-point of the Brillouin zone,

Table 1 Physical parameters used in the theoretical models

	Si	Ge	GaAs	InP
$\alpha(T)(K^{-1})$	2.5×10^{-6} T [4]	5.9×10^{-6} [5]	$-1.43 \times 10^{-12}T^2 + 3.12 \times 10^{-9}T + 5.24 \times 10^{-6}$ [6]	4.56×10^{-6} [6]
B (GP) [7]	97.84	74.70	75.5	72.3
dE_g/dP (10^{-6} eV/bar)	2.9 [7]	5.6 [7]	5.9 [8]	6.2 [8]
E_g (300 K) (eV)	4.27 [7]	4.39 [7]	5.2 [8]	5.2 [8]
N (300 K)[a]	3.57 [9] ($\lambda = 1523$ nm)	4.11 [5] ($\lambda = 1900$ nm)	3.49 [6] ($\lambda = 1523$ nm)	3.17 [6] ($\lambda = 1523$ nm
m_v^* (m_0 units)	0.669 [7]	1.01 [7]	_	_
m_c^*(m_0 units)	0.669 [7]	1.01 [7]	_	_
v_s (m/s) [7]	8430	4920	_	_
T_D (K) [7]	643	348	370	420
C_c (eV) [7]	2.9	5.75	_	_
C_v (eV) [7]	2.9	5.75	_	_
a (Å) [7]	5.4310	5.6579	5.6533	5.8690

[a] Values used for the comparison between the present model and experimental results from Ref. [6], [4] and [5]

because no other accurate values were available. In the same way m_v^* has been considered equal to m_c^*, the density-of-states effective mass in the conduction band. These approximate values of different parameters in Eq. 4 will generally lead to inaccurate predictions of the optical properties of materials, but such approximations do not affect the underlying physical phenomena for the laser-matter interactions. Finally the factor 2 in front of the expression in Eq. 4 corresponds to the degeneracy due to the electronic spin [7]. It should be noted that this model does not consider the optical phonon modes; it considers the acoustic modes [1] and the longitudinal vibrations [10].

Yu-Brooks formalism

A second approach to express the temperature dependence of E_g is to use the Yu-Brooks formalism [10]. The energy gap E_g at the X-point of the Brillouin zone can be expressed in terms of pseudopotential factors, which takes the following form under the Debye-Waller approximation [10]:

$$\frac{1}{E_g}\left(\frac{\partial E_g}{\partial T}\right)_V \approx -2\left|\vec{G}(111)\right|^2 \frac{\partial \bar{B}}{\partial T} \tag{5}$$

where $\vec{G}(111)$ is the reciprocal lattice vector $2\pi\sqrt{3}/a$ and

$$\frac{\partial \bar{B}}{\partial T} = \frac{3\hbar^2 T f(\frac{T_D}{T})}{k_B T_D^3 M} \tag{6}$$

with

$$f(x) = \int_0^x \frac{y^2 \exp(y)}{(\exp(y)-1)^2} dy \tag{7}$$

This formalism, which was originally developed for monatomic semiconductors, has been extended to diatomic semiconductors by Yu and Cardona [1]. For group III–V semiconductors, the mass M is replaced by $(M_{III} + M_V)/2$. For our calculations we also need the Debye temperature. Since the Debye temperature depends on temperature, its value at room temperature is used in this study. As Tsay, Bendow and Mitra [12] pointed out, the Yu-Brooks model considers only the vibrations of the lattice and is independent of the nature of the material. Yu and Cardona [1] showed discrepancies with experimental data when trying to describe the temperature dependence of the energy bandgap. This point will be discussed in section IV.

Model of this study

The lowest point of the conduction band of a direct bandgap material occurs at the same value of k as the highest point of the valence band. A direct optical transition is drawn vertically with no significant change of k, because the absorbed photon has a very small wave vector. The threshold frequency [13, 14] $g\ \omega$ for absorption by the direct transition determines the energy gap $E_g = h\ \omega_g$. The transition of an indirect bandgap material involves both a photon and a phonon because the band edges of the conduction bands are widely separated in k space. The threshold energy for the indirect process is greater than the true band gap. At higher temperatures phonons are already present; if a phonon is absorbed along with a photon, the threshold energy $h\ \omega_g = E_g - h\Omega$, where Ω is the frequency of an emitted phonon of wave [3, 7, 9, 15, 16] vector $K \cong -K_c$.

Now if we plug that value in Eq. 3, we get
For direct bandgap semiconductor [17]

$$\frac{dn}{dT} = \frac{n^2-1}{2n}\left(-3\alpha(T) - \frac{2}{E_g}\frac{1}{1-\frac{E^2}{E_g^2}}\frac{dE_g}{dT}\right) \tag{8}$$

From the above equation we get refractive index of direct bandgap semiconductor as a function of temperature,

$$n(T) = \left[1 + (n(T_{ref})^2 - 1)\right. \\ \left.\exp\left(\int_{T_{ref}}^{T}\left(-3\alpha(T) - \frac{2}{E_g}\frac{1}{1-\frac{E^2}{E_g^2}}\frac{dE_g}{dT}\right)dT\right)\right]^{1/2} \tag{9}$$

Equation 9 can be rewritten for direct bandgap semiconductor as,

$$n(T) = \left[1 + (n(T_{ref})^2 - 1)\right. \\ \left.\exp\left(\int_{T_{ref}}^{T}\left(-3\alpha(T) - \frac{2}{h\omega_g}\frac{1}{1-\frac{E^2}{(h\omega_g)^2}}\frac{d(h\omega_g)}{dT}\right)dT\right)\right]^{1/2} \tag{10}$$

and similarly for indirect bandgap semiconductor we get,

$$(T) = \left[1 + (n(T_{ref})^2 - 1)\right. \\ \exp\left(\int_{T_{ref}}^{T}\left(-3\alpha(T) - \frac{2}{h\omega_g + h\Omega}\right.\right. \\ \left.\left.\frac{1}{1-\frac{E^2}{(h\omega_g+h\Omega)^2}}\frac{d(h\omega_g + h\Omega)}{dT}\right)dT\right)\Bigg]^{1/2} \tag{11}$$

Effect of thermal expansion on the bandgap shift

Thermal expansion causes relative displacement of the valence and conduction bands in semiconductors [18, 19]. This phenomenon can be understood by the following thermodynamic consideration.

$$\left(\frac{\partial E_g}{\partial T}\right)_P = \left(\frac{\partial E_g}{\partial T}\right)_V + \left(\frac{\partial E_g}{\partial V}\right)_T\left(\frac{\partial V}{\partial T}\right)_P \\ = \left(\frac{\partial E_g}{\partial T}\right)_V + \left(\frac{\partial E_g}{\partial P}\right)_T\left(\frac{\partial P}{\partial V}\right)_T\left(\frac{\partial V}{\partial T}\right)_P \tag{12}$$

i.e.

$$\left(\frac{\partial E_g}{\partial T}\right)_P = \left(\frac{\partial E_g}{\partial T}\right)_V - 3\alpha(T)B\left(\frac{\partial E_g}{\partial P}\right)_T \tag{13}$$

With this correction to E_g due to the thermal expansion and noting that we work implicitly at a constant pressure, one can substitute the following expressions for E_g into Eq. 3:

$$\frac{1}{E_g}\frac{dE_g}{dT} = -\frac{3\alpha(T)B}{E_g}\left(\frac{\partial E_g}{\partial P}\right)_T, \quad \text{for the first model} \tag{14}$$

and

$$E_g = E_g^0 - (\Delta E_g)_{electron-lattice} - (\Delta E_g)_{thermal\,expansion} \\ \text{for the second model} \tag{15}$$

with

$$(\Delta E_g)_{thermal\ expansion} = \int_0^T 3\alpha(T)B\left(\frac{\partial E_g}{\partial P}\right)_T dT \tag{16}$$

The effect of the thermal expansion is generally not negligible and has been included in our computations. The values of the bulk modulus (B) and pressure coefficient $[(\partial E_g/\partial P)_T]$ are listed in Table 1.

Experiments

Experimental sources

Theoretical predictions based on the above-mentioned theories have been compared to different experimental data obtained in previous [4–6, 11] studies and in this study. For the diatomic semiconductors GaAs and InP, the refractive index is obtained as a function of temperature by integrating the expression for the thermo-optic coefficient [6] which was given for the wavelength of 1523 nm. The results have been plotted in Figs. 1 and 2. Ge is obtained by first fitting the experimental values [5, 11] of 1/n $\partial n/\partial T$ as a function of temperature and then integrating the resulting

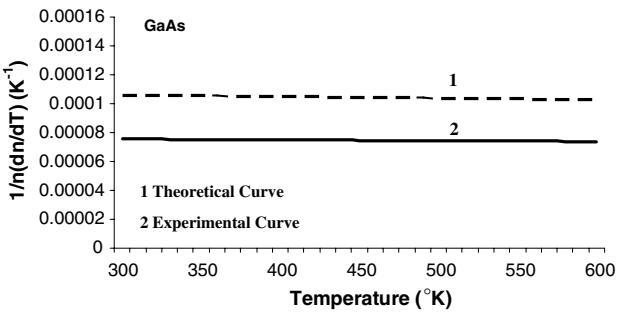

Fig. 1 Refractive index of GaAs between 300 and 600 K at 1523 nm wavelength (experimental results)

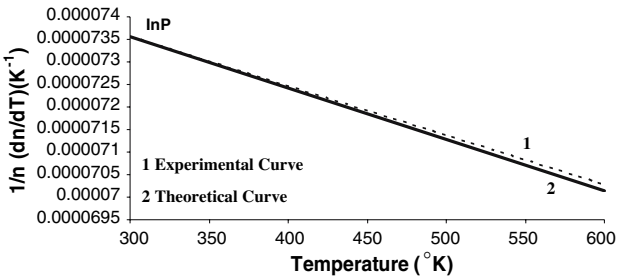

Fig. 2 Refractive index of InP between 300 and 600 K at 1523 nm wavelength (experimental results)

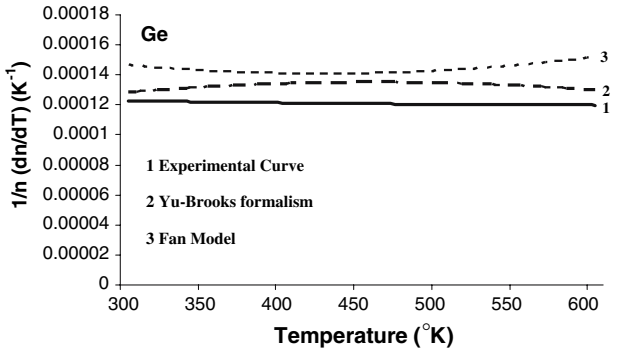

Fig. 3 Refractive index of Ge between 300 and 600 K at 1900 nm wavelength (experimental results)

expression. This yields a straight line (Fig. 3) for the 1/n $\partial n/\partial T$ of Ge as a function of temperature. Similar procedure has been adopted for silicon [4, 11] and its 1/n $\partial n/\partial T$ is plotted in Fig. 4. The coefficients of the curve fits are listed in Table 2.

We have also carried out experimental studies to determine the refractive indices of different semiconductors as a function of temperature. A scheme of the experimental setup is shown in Fig. 5. A Helium–Neon (He–Ne) laser with an output power up to 15 mW at 632.8 nm wavelength was used to irradiate the semiconductor samples which were placed on a stainless steel base heated with an induction heater. This method allows fast heating of the samples without excessive heating of the surrounding fixtures and easy access to the sample for reflectometry. A water cooler was used to prevent melting of the induction tube. The temperature of the sample was measured with a thermocouple.

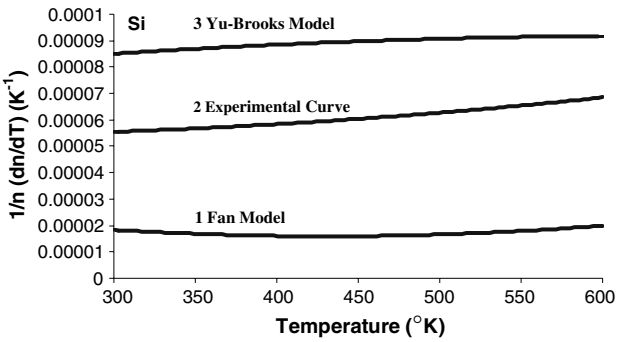

Fig. 4 Refractive index of Si between 300 and 600 K at 1523 nm wavelength (experimental results)

In this experiment, the laser beam is first transmitted through a beam splitter, which is placed between the sample and the He–Ne laser device, and then it irradiates the sample at normal incidence. The beam is reflected by the semiconductor sample toward the beam splitter which directs a portion of the beam to a photodetector. A computer interface was used for data acquisition to collect both the temperature of the sample and the reflected power as functions of time. These data were combined to express the reflected power as a function of temperature, which have been presented in Figs. 6–9 for Si, Ge, GaAs, and InP respectively.

Determination of refractive index

The reflectance of the sample needs to be calculated based on the experimental reflected power in order to obtain the refractive index as a function of temperature. One has to consider the losses on the laser energy due to the beam splitter. Knowing the splitting ratio of the beam splitter and the laser power measured by the photodetector, the total reflected power can be determined. In the present case, only 60% of the incident laser power reached the sample and 40% was reflected by the beam splitter. Then only 40% of the laser power reflected by the sample reached the photodetector. So the reflectivity can be expressed as $R = I/(I_0 \times 0.4 \times 0.6)$, where I is the laser power measured by the photodetector and I_0 is the output power of the He–Ne laser device. I_0 was measured to be 10.7 mW by placing the photodetector directly below the laser device.

Table 2 Polynomial fits of experimental results in Refs [1], [2] and [17]

Semiconductor	$\frac{\partial n}{\partial T}(\mathrm{K}^{-1})$
Si ($\lambda = 1523$ nm)	$-1.49 \times 10^{-10} \times \mathrm{T}^2 + 3.47 \times 10^{-7} \times \mathrm{T} + 9.48 \times 10^{-5}$
Ge ($\lambda = 1900$ nm)	5.057×10^{-4}
GaAs ($\lambda = 1523$ nm)	$-1.86 \times 10^{-10} \times \mathrm{T}^2 + 3.49 \times 10^{-7} \times \mathrm{T} + 1.47 \times 10^{-4}$
InP ($\lambda = 1523$ nm)	$-2.17 \times 10^{-10} \times \mathrm{T}^2 + 3.50 \times 10^{-7} \times \mathrm{T} + 1.15 \times 10^{-4}$

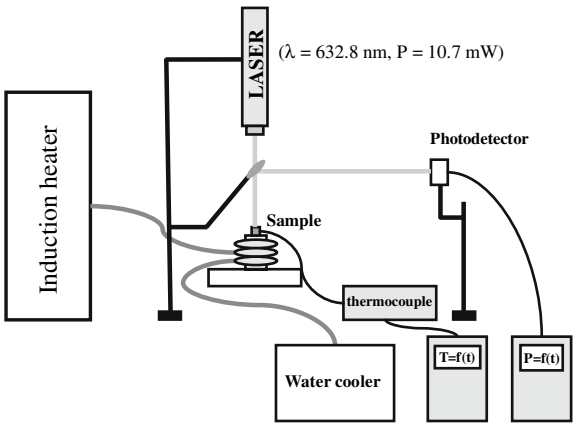

Fig. 5 Experimental setup for reflected power measurement

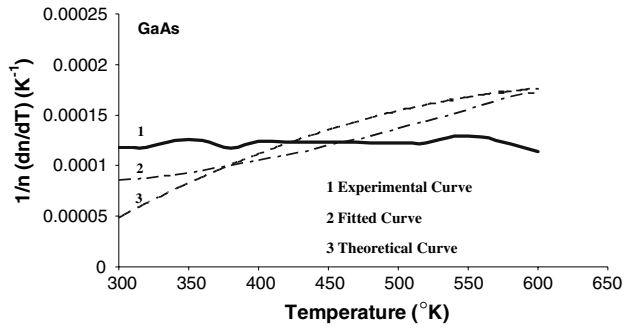

Fig. 6 Refractive index of GaAs between 300 and 600 K at 632.8 nm wavelength

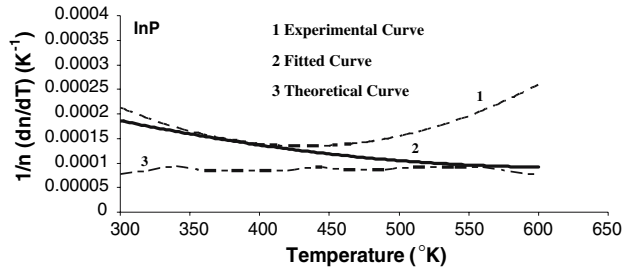

Fig. 7 Refractive index of InP between 300 and 600 K at 632.8 nm wavelength

Finally the refractive index can be calculated using the expression $n = (1 + \sqrt{R})/(1 - \sqrt{R})$ [20] which is based on the Fresnel reflection formula for normal incidence. Both experimental and theoretical values of the refractive index have been obtained for Ge, Si, InP, and GaAs. The samples were cut into thin circular wafers. Their thickness and dopant concentration are listed in Table 3. Every sample was undoped or a low-doped substrate.

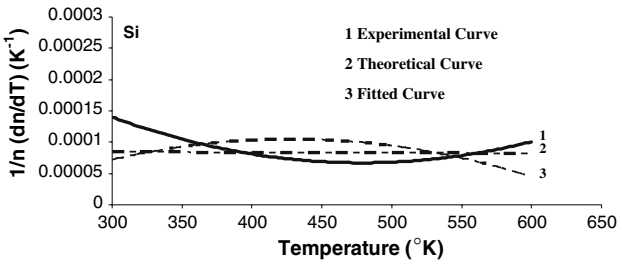

Fig. 8 Refractive index of Si between 300 and 600 K at 632.8 nm wavelength

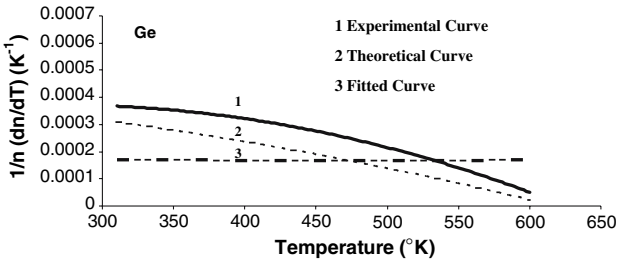

Fig. 9 Refractive index of Ge between 300 and 600 K at 632.8 nm wavelength

Table 3 Basic characteristics of the samples

	Thickness (μm)	Doping concentration (cm^{-3})
Si	690 ± 20	10^{10}
Ge	3970 ± 20	5.1×10^{13}
GaAs	400 ± 20	9.8×10^{7}
InP	400 ± 25	5.1×10^{15}

Comparison with theory

The theoretical values of the refractive index were calculated using the physical parameters listed in Table 1. The values of $n(T)$ obtained from the literature results [4–6] have been compared to the theoretical curves determined by using the Yu-Brooks formalism as shown in Figs. 1–4. The Fan model has also been applied to the monatomic semiconductors Ge and Si to calculate their refractive indices (Figs. 3 and 4). The Fan model agrees well with experiment for Ge. One can, however, notice significant discrepancies for Si, which may be because this model is mostly applicable to insulators and metals. Additionally this model requires the values of different physical properties, such as the effective masses and deformation potentials at the X-point of the Brillouin zone, which are unknown. Accurate values of the deformation potentials and the effective mass of holes are expected to improve the model predictions.

Table 4 Polynomial fits of experimental results at 632.8 nm wavelength (This work)

Semiconductor	$\frac{\partial n}{\partial T}(\mathrm{K}^{-1})$
Si	$3.020 \times 10^{-7} \times \mathrm{T} + 2.858 \times 10^{-4}$
Ge	$4.218 \times 10^{-5} \times \mathrm{T} - 1.305 \times 10^{-2}$
GaAs	$1.195 \times 10^{-6} \times \mathrm{T} - 8.952 \times 10^{-5}$
InP	$-8.095 \times 10^{-7} \times \mathrm{T} + 7.555 \times 10^{-4}$

The Yu-Brooks formalism provides better agreement between the theory and experiment for Si and Ge, and satisfactory results for InP. For GaAs, however, the theory and experimental data differ by about 15% at 600 K. This discrepancy may be due to the effect of "self-energy" on the temperature dependence of the energy bandgap, [7, 9] which has not been considered in this work. This effect generally reduces the energy gap and thus decreases the refractive index. Yu and Cardona [1] observed discrepancy in their results for the energy gap due to this effect.

The refractive indices obtained from the experimental data of the present work are slightly smaller than those obtained from the literature [12]. This is mainly due to the uncertainties over the percentages of transmitted and reflected light in the beam splitter and the spectral width of the He–Ne laser used in this study. The refractive indices have been fitted to second-order polynomials and then deduced empirical equations of the thermo-optic coefficients are deduced as listed in Table 4. For each sample the experimental refractive indices have been compared to the theoretical values obtained from the Yu-Brooks formalism (Figs. 6–9). While deriving the expressions for $n(T)$ by integrating the expressions for the thermo-optic coefficients, the initial condition to determine the constant of integration was taken as the value of the refractive index at 300 K. This initial condition was obtained from the reflectometry data at 300 K. Although the theoretical and experimental values compare well for GaAs and Si, there is a difference of about 15% for Ge and InP at 600 K. We noticed in our study that the variation of the experimental refractive index with temperature depended strongly on the crystallographic plane and polishing of the sample surface. Additionally the concentration of free electrons, whose effect generally is not taken into account because of its low level, may also influence the thermo-optic coefficient.

Conclusion

A model is presented for the temperature dependence of the refractive index based on the Lorentz model with a single-oscillator approximation. The model also employs the Debye-Waller approximation for the temperature dependence of the energy bandgap. The bandgap is taken equal to the X-point of the Brillouin zone. Considering the simplicity of the model, it compares well with experimental results. Some discrepancies, however, are observed for two samples (InP and Ge) which may be due to the crystallographic plane of the sample surface and the amount of impurity in the sample. The discrepancies could also be due to the scattering (damping) effect in the material and the self-energy effect on the shift of the energy gap with temperature, which have been neglected in this model.

References

1. Yu PY, Cardona M (1970) Phys Rev 2:3193
2. Fan HY (1951) Phys Rev 82:900
3. Tsay YF, Mitra SS, Bendow B (1974) Phys Rev B 10:1476
4. Della Corte G, Cocorullo G, Rendina I (1999) Phys Rev 74:1613
5. Ghosh G (1998) Handbook of thermo-optic coefficients of optical materials with applications. Academic Press
6. Della Corte FG, Cocorullo G, Iodice M, Rendina I (2000) Appl Phys Lett 77:1614
7. Allen PB (1978) Phys Rev B 18:5217; Chakraborty B, Allen PB (1978) Phys Rev B 18:5225
8. Yu SC (1964) PhD thesis. Harvard University (unpublished)
9. Kim CK, Lautenschlager P, Cardonam M (1986) Solid State Commun 59:797
10. Haug A (1972) Theoretical solid state physics, vol 1 and 2. Pergamon Press
11. McCaulley JA, Donnelly VM, Vernon M, Taha I (1994) Phys Rev B 49:7408
12. Tsay YF, Bendow B, Mitra SS (1973) Phys Rev B 8:2688
13. Wolf HF (1969) Silicon semiconductor data. Pergamon Press, Oxford
14. Engineering Physics 3F3, Experiment#2
15. Adachi S (2005) Properties of Group-IV, III–V and II–VI semiconductors. Wiley
16. Magunov AN (1992) Opt Spectrosc 73:205
17. Chakravarty A, Quick NR, Kar A (2007) J Appl Phys 102:073111
18. Lourenço SA, Dias IFL, Duarte JL, Laureto E, Poças LC, Toginho Filho DO, Leite JR (2004) Braz J Phys 34:517
19. Lautenschlager P, Garriga M, Vina L, Cardona M (1987) Phys Rev B 36:4821
20. Fröhlich H (1950) Phys Rev 79:845